J Pharmacol Sci **110**, 370 – 380 (2009)

Journal of Pharmacological Sciences

Full Paper

Inhibition of Lipid Infusion–Induced Skeletal Muscle Insulin Resistance by Cotreatment With Tempol and Glutathione in Mice

Byung Seok Kim[1], Hye-Na Cha[2,3], Yong-Woon Kim[2], Jong-Yeon Kim[2], Jin-Myoung Dan[4], and So-Young Park[2,3]

[1]*Department of Internal Medicine, Catholic University of Daegu, Daegu, 700-443, Korea*
[2]*Department of Physiology, College of Medicine,* [3]*Aging-associated Vascular Disease Research Center, Yeungnam University, Daegu, 705-717, Korea*
[4]*Department of Orthopedic Surgery, Gumi CHA University Hospital, Gumi, 730-728, Korea*

Received February 12, 2009; Accepted May 21, 2009

Abstract. In the present study, we examined whether lipid infusion–induced insulin resistance in skeletal muscle could be reversed by the antioxidants tempol, glutathione (GSH), or tempol with GSH in male C57BL/6J mice via hyperinsulinemic-euglycemic clamp. Lipid infusion increased the mRNA level of mitochondrial type superoxide dismutase (Mn-SOD), glutathione peroxidase 1, tumor necrosis factor-α, and interleukin-6. Lipid infusion decreased GSH and GSH/glutathione disulfide (GSSG) ratio and increased the activities of JNK and p38 in skeletal muscle. Lipid infusion induced insulin resistance in whole body and skeletal muscle. Treatment with the SOD mimetic tempol did not prevent oxidative stress, the inflammatory response, and insulin resistance induced by lipid infusion. Tempol alone increased oxidative stress and aggravated the lipid-induced inflammatory response. GSH at 100 and 200 μmol$\cdot$kg$^{-1}\cdot$h^{-1} did not prevent insulin resistance and the inflammatory response by lipid infusion. On the contrary, GSH at 100 μmol$\cdot$kg$^{-1}\cdot$h^{-1} with tempol prevented insulin resistance in the whole body and skeletal muscle, and it completely reversed oxidative stress and the inflammatory response. These results suggest that lipid infusion–induced insulin resistance in skeletal muscle is produced by oxidative stress and cotreatment with tempol and GSH inhibits lipid-induced insulin resistance.

Keywords: insulin resistance, lipid, oxidative stress, skeletal muscle, inflammation

Introduction

Insulin resistance, defined as decreases in insulin sensitivity and/or responsiveness to promote glucose disposal in peripheral tissues, plays an important role in the pathogenesis of non-insulin dependent diabetes mellitus (1, 2).

Many factors have been demonstrated to induce insulin resistance in vivo and in vitro including lipid-derived free fatty acids (FFAs) (3, 4). In addition to chronic increase of FFAs by a high fat diet, acute and relatively short-term lipid infusion also produces insulin resistance in rodents and humans (5 – 8). Intravenous infusion of 20% intralipid for 2 h induces skeletal muscle insulin resistance (9). The underlying mechanisms responsible for fatty acid–induced insulin resistance have been investigated for more than forty years since Randle et al. demonstrated that FFAs compete with glucose for oxidative phosphorylation (10). Recently, however, fatty acid metabolites, oxidative stress, and pro-inflammatory cytokines have received more attention as possible mediators of lipid-induced insulin resistance (11).

Although the physiological role of reactive oxygen species (ROS) in cellular signaling pathways have been reported, increased production of ROS or/and reduced capacity of their elimination, termed oxidative stress, induces tissue damage (12, 13). Previous studies have claimed that acute increase of FFAs by lipid infusion induced oxidative stress and whole body insulin resistance via activation of c-Jun N-terminal kinase (JNK) (6, 14, 15). Oxidative stress also activates the IκB kinase (IKK) / nuclear factor-κB (NF-κB) system to

*Corresponding author. sypark@med.yu.ac.kr
Published online in J-STAGE
doi: 10.1254/jphs.09046FP

produce pro-inflammatory cytokines, such as tumor necrosis factor-α (TNF-α) and interleukin-6 (IL-6), which are also responsible for insulin resistance (15). However, not all the research agrees with the negative role of ROS in terms of glucose metabolism in skeletal muscle. Indeed, some studies have shown ROS to have a stimulatory effect on glucose uptake under various experimental conditions. Increased ROS generation by muscle contraction stimulates glucose uptake through AMP-activated protein kinase (AMPK) activation in mice (16). Incubation of isolated muscle with H_2O_2 increases glucose uptake through a phosphatidylinositol 3-kinase–dependent mechanism (16, 17).

The first line of defense against ROS-mediated tissue damage comprises several antioxidant enzymes including superoxide dismutase (SOD), catalase, and glutathione peroxidase (GPx) (18, 19). SOD, including mitochondrial type Mn-SOD and cytosolic type Cu/Zn-SOD, can provide antioxidant protection by inactivating O^{-}_2, and preventing O^{-}_2 from forming more destructive ROS such as peroxynitrite and ·OH (15, 19). In skeletal muscle, the mitochondrial respiratory chain continuously produces O^{-}_2, which is accelerated by the oversupply of FFAs. The generated O^{-}_2 can be converted to less harmful H_2O_2 by SOD (20). H_2O_2 is then scavenged by GPx that converts H_2O_2 to H_2O through oxidizing glutathione (GSH) to glutathione disulfide (GSSG) (21, 22). GSH is then regenerated from GSSG by glutathione reductase (GRx) (23). Antioxidants such as the SOD mimetic tempol and GSH have been used for the treatment of a variety of diseases (24 – 26).

Therefore, in this study, we investigated whether the SOD mimetic tempol and GSH can reverse acute lipid infusion–induced insulin resistance in skeletal muscle of mice via the hyperinsulinemic-euglycemic clamp technique.

Materials and Methods

Animals

Male C57BL/6J mice were housed in the animal unit of the College of Medicine at Yeungnam University. Mice were housed in a group cage in a room that was on a 12:12-h light/dark cycle, lights-on at 7:00 and lights-off at 19:00. The mice were fed on a standard chow diet and given ad libitum access to water. This study was conducted in accordance with the guidelines for the care and use of laboratory animals provided by Yeungnam University, and all experimental protocols were approved by the ethical committee of Yeungnam University.

Surgery for catheterization

Four days before the experiments, mice were anesthetized by intraperitoneal injection of a combination of anesthetics (25 mg/kg body weight, tiletamine and zolezepam; 10 mg/kg body weight, xylazine), and a catheter (silicone tubing; Helix Medical, Carpinteria, CA, USA) was inserted in the right internal jugular vein. On the day of the experiment, a Y connector was attached to the jugular vein catheter to intravenously deliver solutions (glucose and insulin).

Intravenous infusions

After an overnight fast, mice in the awake state were placed in a rat-size restrainer and tail restrained using a tape to obtain blood samples from the tail vessels. Intralipid (20%) with 33 U/ml heparin was infused for 2 h before and during the clamp procedure at 3.3 μl/min in the lipid-infused group and saline was infused in the saline-infused group. Intralipid is composed of 20% soybean oil, 1.2% egg yolk phospholipids, 2.25% glycerin, and water (Fresenius Kabi Korea, Cheonan, Korea). Tempol at the rate of 16 $\mu mol \cdot kg^{-1} \cdot min^{-1}$ was infused with either the lipid or saline before and during clamp for 4 h. GSH at 100 (GSH100) and 200 (GSH200) $\mu mol \cdot kg^{-1} \cdot h^{-1}$ and GSH100 with tempol were infused with the lipid before and during clamp. GSH100 and GSH100 with tempol were infused with saline as a control. For the time-course effect of lipid on inflammation and oxidative stress of skeletal muscle, lipid was infused with 33 U/ml heparin for 0, 0.5, 1, 2, and 3 h at 3.3 μl/min.

Hyperinsulinemic-euglycemic clamp

Hyperinsulinemic euglycemic clamps: For a 2-h hyperinsulinemic euglycemic clamp, human insulin (Novolin; Novo Nordisk, Bagsvaerd, Denmark) was continuously infused at a rate of 15 $pmol \cdot kg^{-1} \cdot min^{-1}$ to raise plasma insulin. Blood samples (20 μl) were collected by using a capillary tube at 20-min intervals for the immediate measurement of plasma glucose concentration, and 20% glucose was infused at variable rates to maintain glucose at constant concentration. Basal and insulin-stimulated rates of whole body glucose uptake were estimated with a continuous infusion of [3-^{3}H]glucose (PerkinElmer Life and Analytical Sciences, Waltham, MA, USA) for 2 h before the clamps (0.05 μCi/min) and throughout the clamps (0.1 μCi/min), respectively (27). To estimate insulin-stimulated glucose uptake in individual tissues, 2-deoxy-D-[1-^{14}C]glucose (2-[^{14}C]DG, PerkinElmer Life and Analytical Sciences) was administered as a bolus (10 μCi) at 75 min after the start of the clamps (27). At the end of the clamps, mice were anesthetized, and tissues were dissected and stored at –80°C until

biochemical and molecular analysis.

Biochemical assays: Plasma glucose concentration was measured using a Beckman Glucose Analyzer 2 (Beckman, Fullerton, CA, USA), and plasma insulin concentration was measured using enzyme-linked immunosorbent assay (Linco Research, St. Charles, MO, USA). Plasma triglyceride and free fatty acids were determined by enzymatic colorimetric methods (Sigma, St. Louis, MO, USA). Plasma concentrations of [3-^{3}H]glucose, 2-[^{14}C]DG, and $^{3}H_2O$ were determined after deproteinization of plasma samples (27). For the determination of tissue 2-[^{14}C]DG 6-phosphate (2-[^{14}C]DG-6-*P*) content, tissue samples were homogenized, and the supernatants were subjected to an ion exchange column to separate 2-DG-6-*P* from 2-DG (27).

Calculations: Rate of insulin-stimulated whole body glucose uptake was determined as the ratio of the [^{3}H]glucose infusion rate [disintegrations per minute (dpm/min)] to the specific activity of plasma glucose (dpm/μmol) during the final 30 min of clamps. Because 2-DG is a glucose analog that is phosphorylated but not metabolized, insulin-stimulated glucose uptake in individual tissues can be estimated by determining the tissue content of 2-[^{14}C]DG-6-*P*. On this basis, glucose uptake in individual tissues was calculated from the plasma 2-[^{14}C]DG profile, which was fitted with a double exponential or linear curve by using MLAB (Civilized Software, Bethesda, MD, USA) and tissue 2-[^{14}C]DG-6-*P* content.

Real-time PCR

Skeletal muscle (about 40 mg) was homogenized in TRI reagent (Sigma) using an Ultra-Turrax T25 (Janke & Kunkel, IKA-Labortechnik, Staufel, Germany). RNA was reverse transcribed to cDNA from 1 μg of total RNA by using High-Capacity cDNA Reverse Transcription Kits (Applied Biosystems, Foster City, CA, USA). Quantitative real-time PCR was performed using the Real-Time PCR 7500 Software system and Power SYBR Green PCR master mix (Applied Biosystems), according to the manufacturer's instructions. The reactions were incubated at 95°C for 10 min, followed by 45 cycles at 95°C for 15 s, 55°C for 20 s, and 72°C for 35 s. Expression levels of β-actin were used for sample normalization. Primers for mouse β-actin, TNF-α, IL-6, SOD, and GPx were based on NCBI's Nucleotide database and designed using the Primer Express program (Applied Biosystems): β-actin (121 bp: forward, 5'-TGG ACA GTG AGG CAA GGA TAG-3'; reverse, 5'-TAC TGC CCT GGC TCC TAG CA-3'), TNF-α (71 bp: forward, 5'-CTA TCT CCA GGT TCT CTT CAA-3'; reverse, 5'-GCA GAG AGG AGG TTG ACT TTC), IL-6 (71 bp: forward, 5'-AAA TGA TGG ATG CTA CCA AAC T-3'; reverse, 5'-CCA GAA GAC CAG AGG AAA TTT T-3'), SOD (71 bp: forward, 5'-CTG CTC TAA TCA GGA CCC ATT-3'; reverse, 5'-GTG CTC CCA CAC GTC AAT C-3'), GPx1 (71 bp: forward, 5'-GAA GTG CGA AGT GAA TGG TG-3'; reverse, 5'-TGG GTG TTG GCA AGG C-3').

Western blotting

Skeletal muscle samples were used for measurement of phosphorylated extracellular regulated kinase (pERK), ERK, p-p38, p38, JNK, and p-JNK. Muscles (about 40 mg) were homogenized in a lysis buffer (Invitrogen, Carlsbad, CA, USA) containing 1% NP40, 150 mM NaCl, 5 mM MgCl, 10 mM HEPES, leupeptin, and pepstatin A. A 60-μg sample of the total protein per lane was separated by 12% SDS-polyacrylamide gel electrophoresis. The protein was then transferred to a PVDF membrane (0.45 μm; Gelman Laboratory, Ann Arbor, MI, USA). After blocking with 5% skin milk / 10 mM Tris-HCl, pH 7.4 / 150 mM NaCl / 0.1% Tween 20, the membrane was incubated overnight at 4°C with the primary antibodies (diluted 1:1000). The specific antibody binding was detected using sheep anti-rabbit IgG horseradish peroxidase (1:2000; Santa Cruz Biotechnology, Santa Cruz, CA, USA) for 1 h at room temperature and visualized using an enhanced chemiluminescence detection regent (Amersham Biosciences, Westborough, MA, USA).

GSH and GSH/GSSG ratio

Total GSH and oxidized GSSG were measured using a Bioxytech GSH/GSSG-412 assay kit (OxisResearch, Foster City, CA, USA). Skeletal muscle (about 50 mg) was diluted 10 times using 50 mM phosphate buffer (pH 7) containing 1 mM EDTA, and homogenized and then centrifuged at 10,000 × *g* for 15 min (4°C). For oxidized GSSG measurements, 50 μl of the supernatant was mixed with 5 μl of 1-methyl-2-vinylpyridium trifluorlmethanesulfonate (OxisResearch) to prevent GSH oxidation. After the addition of 50 μl of 10% metaphosphoric acid (OxisResearch), the sample mixture was centrifuged at 5000 × *g* for 5 min. Then, 50 μl of supernatant was mixed with 700 μl of GSSG buffer (OxisResearch) and the assay was performed according to the manufacturer's instructions. For total GSH, 100 μl of supernatant was mixed with 100 μl of 10% metaphosphoric acid and then centrifuged at 5000 × *g* for 5 min. Then 50 μl of supernatant was mixed with 3 ml of GSH buffer (OxisResearch). The assay was performed according to the manufacturer's instructions. GSH and GSH/GSSG ratio were used as markers for oxidative stress.

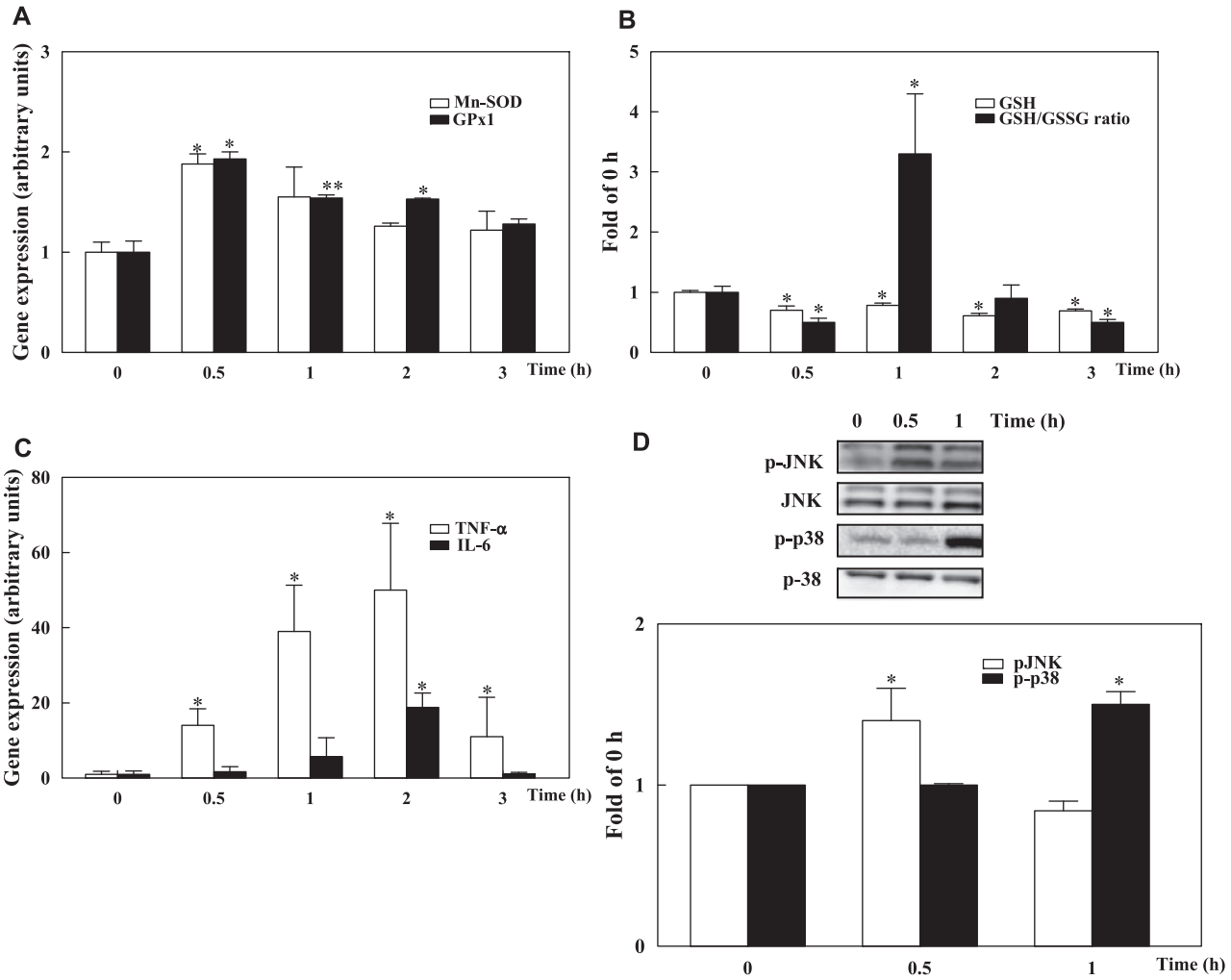

Fig. 1. Effect of lipid infusion on the gene expression, oxidative stress markers, and phosphorylation of mitogen-activated protein kinase subfamily in skeletal muscle. Intralipid (20%) was infused intravenously for 0, 0.5, 1, 2, and 3 h. Gene expression of antioxidant enzymes, mitochondrial type superoxide dismutase (Mn-SOD) and glutathione peroxidase 1 (GPx1) (A). Concentration of oxidative stress markers, total glutathione (GSH), and total GSH/oxidized glutathione disulfide (GSSG) ratio (B). Gene expression of tumor necrosis factor-α (TNF-α) and interleukin-6 (IL-6) (C). Phosphorylation of JNK and p38 (D). Values are each the mean ± S.E.M. of 3 – 4 experiments. *P<0.05 vs. corresponding value at 0 h.

Statistics

The results are each expressed as the mean ± S.E.M. The difference between two groups was assessed by Student's *t*-test and the difference between three or more groups was analyzed by ANOVA with a post-hoc analysis by a Duncan's multiple test. A P value <0.05 was considered significant.

Results

Lipid infusion induced oxidative stress and inflammatory response

In order to determine whether lipid induces oxidative stress, we measured the expression of the antioxidant enzymes Mn-SOD and GPx1 and the markers for oxidative stress, GSH and GSH/GSSG ratio, in the skeletal muscle of lipid-infused mice for 0, 0.5, 1, 2, and 3 h. Lipid infusion increased the mRNA expression of Mn-SOD at 0.5 h and GPx1 at 0.5, 1, and 2 h in skeletal muscle (Fig. 1A). GSH level was decreased by lipid infusion at 0.5, 1, 2, and 3 h; and GSH/GSSG ratio was reduced at 0.5 and 3 h, but showed an increase at 1 h (Fig. 1B). We speculate that the increased synthesis or activity of antioxidant enzymes temporarily overcomes oxidative stress at the 1-h point of time. Next, the gene expression of pro-inflammatory cytokines and the activities of a mitogen-activated protein kinase (MAPK) subfamily were measured in the skeletal muscle of mice. The mRNA level of TNF-α was increased at 0.5, 1, 2, and 3 h, and the mRNA level of

Table 1. Metabolic parameters during basal and clamp periods in various groups

		N	Body weight (g)	Basal period		Clamp period	
				plasma glucose (mM)	plasma insulin (pM)	plasma glucose (mM)	plasma insulin (pM)
Saline	control	5	21 ± 0.3	6.9 ± 0.26	31 ± 1.0	6.9 ± 0.43	85 ± 6.1
	tempol	5	21 ± 0.2	7.8 ± 0.84	47 ± 8.7	6.4 ± 0.17	99 ± 10.6
Lipid	control	5	21 ± 0.6	6.7 ± 0.08	87 ± 39.1	7.0 ± 0.34	223 ± 17.4*
	tempol	5	21 ± 0.5	6.3 ± 0.22	84 ± 44.2	7.6 ± 0.30	191 ± 22.1*

Tempol was infused at 16 μmol·kg^{-1}·min^{-1}. Values are expressed as the mean ± S.E.M. N indicates the number of experimental cases. *P<0.05 vs. saline-infused control.

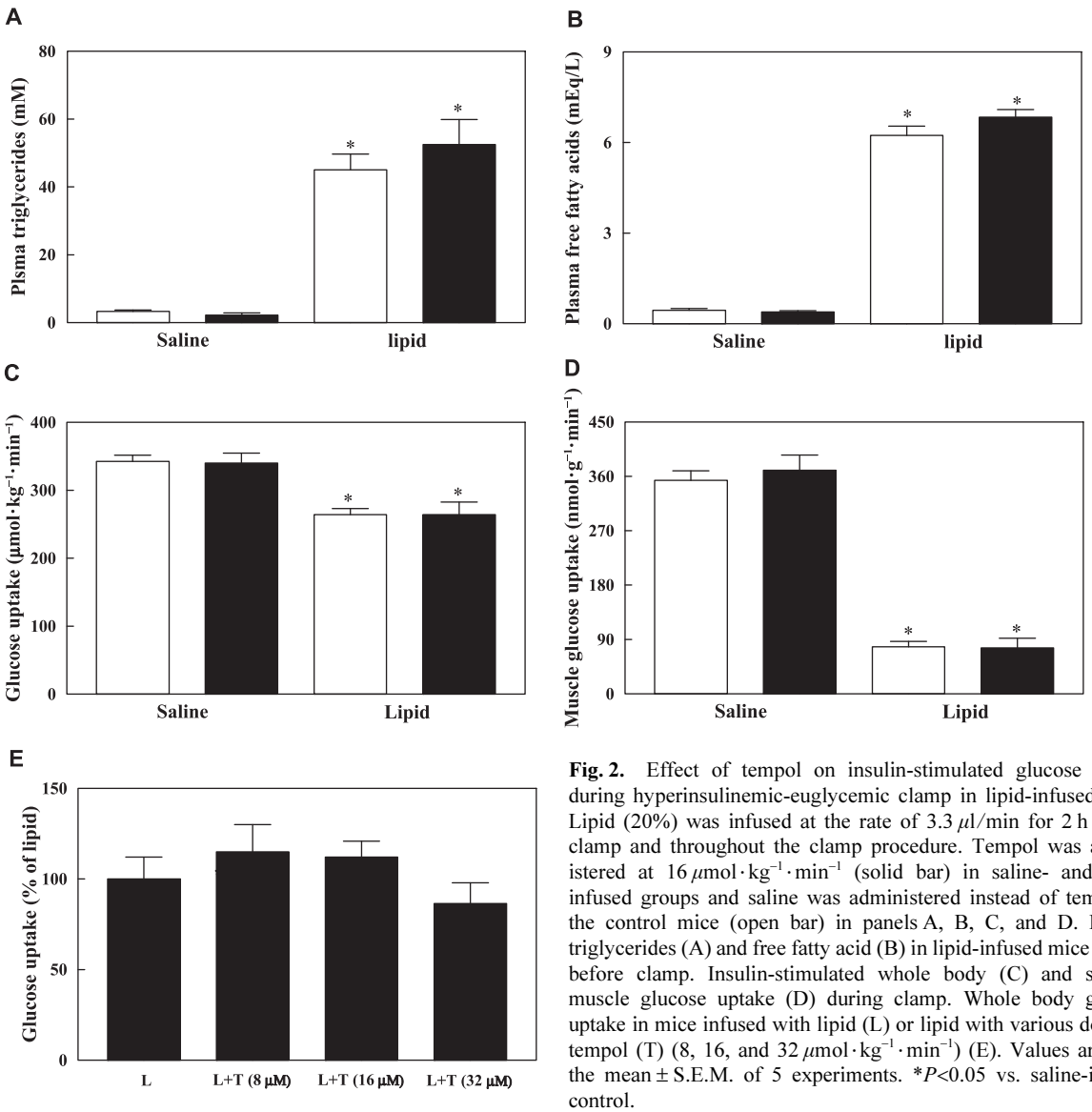

Fig. 2. Effect of tempol on insulin-stimulated glucose uptake during hyperinsulinemic-euglycemic clamp in lipid-infused mice. Lipid (20%) was infused at the rate of 3.3 μl/min for 2 h before clamp and throughout the clamp procedure. Tempol was administered at 16 μmol·kg^{-1}·min^{-1} (solid bar) in saline- and lipid-infused groups and saline was administered instead of tempol in the control mice (open bar) in panels A, B, C, and D. Plasma triglycerides (A) and free fatty acid (B) in lipid-infused mice for 2 h before clamp. Insulin-stimulated whole body (C) and skeletal muscle glucose uptake (D) during clamp. Whole body glucose uptake in mice infused with lipid (L) or lipid with various doses of tempol (T) (8, 16, and 32 μmol·kg^{-1}·min^{-1}) (E). Values are each the mean ± S.E.M. of 5 experiments. *P<0.05 vs. saline-infused control.

IL-6 was increased at 2 h in lipid infused mice (Fig. 1C). Activity of the MAPK subfamily was determined by phosphorylation of JNK, p-38, and ERK by Western blotting. While lipid increased the activities of JNK and p-38 in skeletal muscle (Fig. 1D), ERK was not increased by lipid infusion (data not shown). These

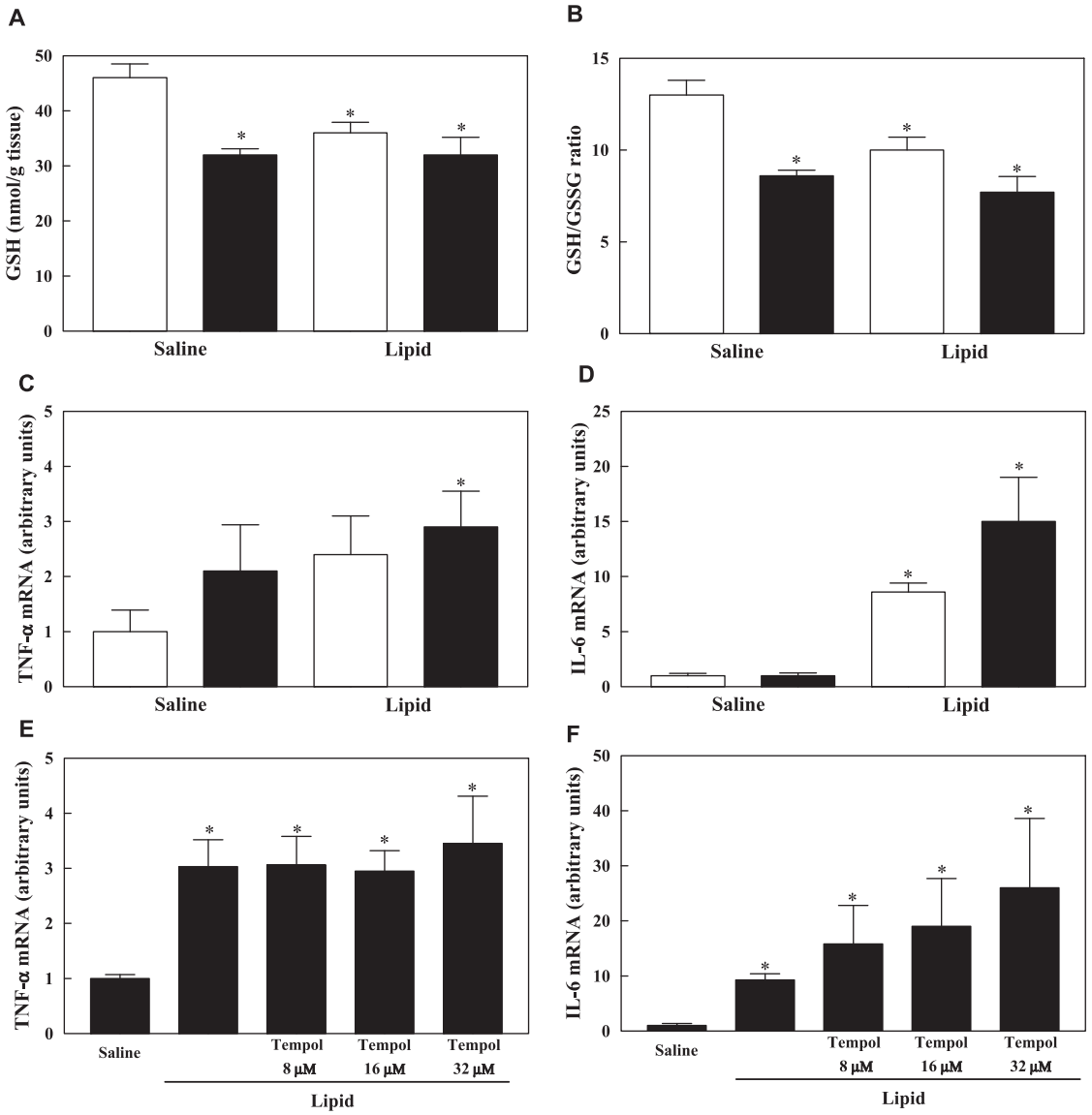

Fig. 3. Effect of tempol on oxidative stress markers and the gene expression of cytokines in skeletal muscle of lipid-infused mice at the end of 2-h clamp. Lipid (20%) was infused at the rate of 3.3 μl/min for 2 h before clamp and throughout the clamp procedure. Tempol was administered at 16 μmol·kg^{-1}·min^{-1} (solid bar) in saline- and lipid-infused groups and saline was administered instead of tempol in the control mice (open bar) in panels A, B, C, and D. Total glutathione (GSH) concentration (A). Total GSH/oxidized glutathione disulfide (GSSG) ratio (B). Gene expression of tumor necrosis factor-α (TNF-α) (C) and interleukin-6 (IL-6) (D). Gene expression of TNF-α (E) and IL-6 (F) in mice infused with lipid or lipid with various doses of tempol (8, 16, and 32 μmol·kg^{-1}·min^{-1}). Gene expression of cytokines is presented as fold increase of the saline control. Values are each the mean ± S.E.M. of 5 experiments. *P<0.05 vs. saline-infused control.

results suggest that lipid infusion increases oxidative stress, the inflammatory response, and the activity of MAPK.

Heparin affects lipid metabolism (28) that may influence insulin sensitivity in mice. Therefore, we measured the plasma lipid levels and insulin sensitivity in mice infused with 33 U/ml heparin at 3.3 μl/min, which was the concentration used in lipid-induced insulin resistance experiments. Insulin sensitivity and the plasma levels of triglyceride and free fatty acids were not affected by heparin (data not shown).

Tempol did not prevent oxidative stress and insulin resistance

Initially, we studied the effect of the SOD mimetic tempol on oxidative stress and insulin resistance by lipid infusion. Tempol treatment did not affect plasma concentrations of glucose, insulin, triglycerides, and

Table 2. Metabolic parameters during basal and clamp periods in various groups

		N	Body weight (g)	Basal period		Clamp period	
				plasma glucose (mM)	plasma insulin (pM)	plasma glucose (mM)	plasma insulin (pM)
Saline	control	6	21 ± 0.6	6.0 ± 0.77	50 ± 1.0	7.0 ± 0.30	138 ± 8.1
	GSH100	6	22 ± 1.0	5.8 ± 0.39	52 ± 1.7	6.4 ± 0.29	156 ± 14.9
	GSH100 + tempol	4	20 ± 0.4	5.2 ± 0.24	49 ± 2.7	7.2 ± 0.33	169 ± 11.8
Lipid	control	7	22 ± 0.9	5.6 ± 0.27	68 ± 7.4*	6.6 ± 0.35	294 ± 45.4*
	GSH100	4	22 ± 1.0	5.5 ± 0.37	65 ± 7.5*	5.8 ± 0.68	321 ± 24.6*
	GSH200	4	22 ± 0.6	5.5 ± 0.68	61 ± 5.4*	6.3 ± 0.40	374 ± 28.7*
	GSH100 + tempol	8	23 ± 1.1	5.3 ± 0.50	74 ± 8.9*	6.6 ± 0.42	369 ± 93.0*

Glutathione (GSH) was infused at 100 (GSH100) or 200 (GSH200) μmol·kg^{-1}·h^{-1}. Tempol was infused at 16 μmol·kg^{-1}·min^{-1}. Values are expressed as the mean ± S.E.M. N indicates the number of experimental cases. *P<0.05 vs. saline-infused control.

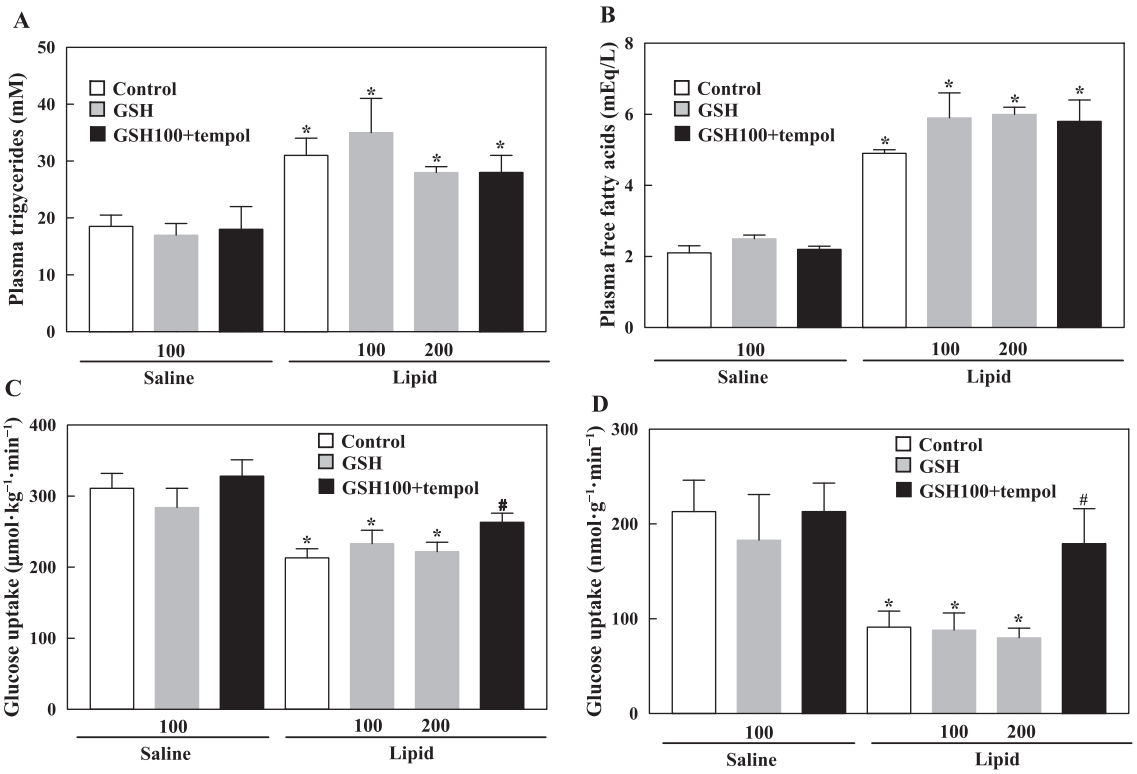

Fig. 4. Effect of glutathione (GSH) and GSH with tempol on insulin-stimulated glucose uptake during hyperinsulinemic-euglycemic clamp in lipid-infused mice. Mice were in The lipid-infused mice were administered GSH at 100 (GSH100) and 200 (GSH200) μmol·kg^{-1}·h^{-1} or GSH100 with tempol (16 μmol·kg^{-1}·min^{-1}). In the saline-infused group, GSH was administered at 100 μmol·kg^{-1}·h^{-1}. Lipid (20%) was infused at the rate of 3.3 μl/min for 2 h before clamp and throughout the clamp procedure. Plasma triglycerides (A) and free fatty acid (B) in lipid-infused mice for 2 h before clamp. Insulin-stimulated whole body (C) and skeletal muscle glucose uptake (D) during clamp. Values are each the mean ± S.E.M. of 4 – 8 experiments. *P<0.05 vs. saline-infused control. $^{\#}P$<0.05 vs. lipid-infused control.

FFAs. Lipid infusion for 2 h before clamp increased plasma concentrations of triglycerides and FFAs (Table 1 and Fig. 2).

During clamp experiments, plasma glucose concentration was maintained at approximately 7 mM. Plasma insulin concentrations were significantly higher in both lipid- and lipid with tempol–infused mice compared with saline-infused control mice, although insulin was infused at the same rate in all four groups (Table 1). Increased insulin levels in lipid-infused mice may be

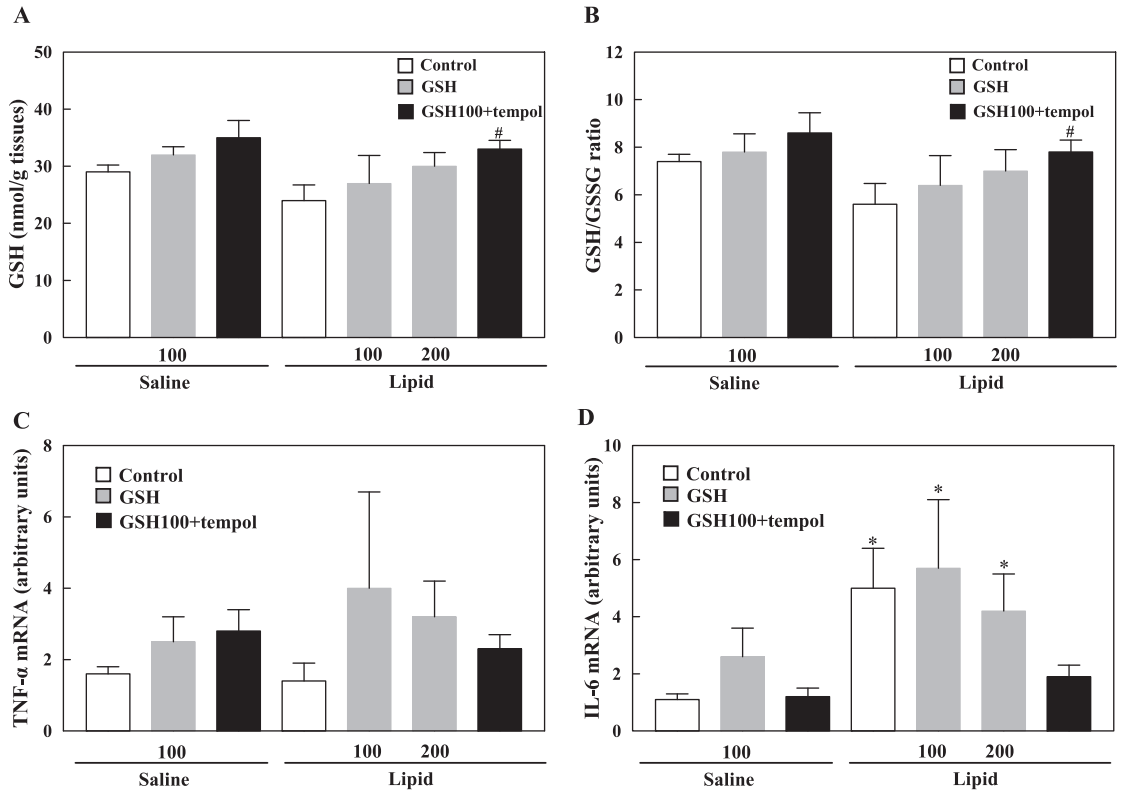

Fig. 5. Effect of glutathione (GSH) and GSH with tempol on oxidative stress markers and the gene expression of cytokines in skeletal muscle of lipid-infused mice at the end of 2-h clamp. The lipid-infused mice were administered GSH at 100 (GSH100) and 200 (GSH200) μmol·kg^{-1}·h^{-1} or GSH100 with tempol (16 μmol·kg^{-1}·min^{-1}). In the saline-infused group, GSH was administered at 100 μmol·kg^{-1}·h^{-1}. Lipid (20%) was infused at the rate of 3.3 μl/min for 2 h before clamp and throughout the clamp procedure. Total glutathione (GSH) concentration (A). Total GSH/oxidized glutathione disulfide (GSSG) ratio (B). Gene expression of tumor necrosis factor-α (TNF-α) (C) and interleukin-6 (IL-6) (D). Values are each the mean ± S.E.M. of 4 – 8 experiments. *P<0.05 vs. saline-infused control. $^{\#}P$<0.05 vs. lipid-infused control.

caused by increased endogenous insulin secretion and delayed clearance of insulin in the liver (29). Insulin-stimulated glucose uptake in the whole body and skeletal muscle did not change after tempol infusion, while they were significantly decreased by lipid infusion, suggesting that lipid infusion induces whole body and skeletal muscle insulin resistance. However, coinfusion with lipid and tempol did not prevent insulin resistance (Fig. 2). Tempol, lipid, or lipid with tempol reduced GSH and the GSH/GSSG ratio (Fig. 3). Lipid or lipid with tempol significantly increased the mRNA level of TNF-α and IL-6 (Fig. 3). These results suggest that tempol increased oxidative stress rather than decreased it and did not prevent lipid-infused insulin resistance.

GSH with tempol prevented oxidative stress, inflammation, and insulin resistance

Next, the effect of cotreatment with GSH and tempol was tested since these two antioxidants have different roles in scavenging ROS. GSH was infused at GSH100 and GSH200. GSH, tempol, or GSH with tempol did not affect plasma concentrations of glucose and insulin in saline-infused or lipid-infused mice compared with the corresponding control mice. Lipid infusion increased plasma concentrations of insulin, although plasma glucose concentrations remained unaltered (Table 2). Plasma concentrations of triglyceride and FFAs were markedly increased by lipid infusion, while GSH, tempol, or GSH with tempol did not affect them (Fig. 4).

Insulin stimulated whole body glucose uptake did not change after treatment with GSH100 or GSH100 and tempol, in the saline-infused group. Lipid infusion significantly reduced insulin stimulated whole body glucose uptake that was reversed by GSH100 with tempol treatment. GSH100 and GSH200 did not prevent lipid-infused insulin resistance. The rate of insulin stimulated glucose uptake in skeletal muscle was significantly reduced by lipid infusion compared with saline-infused control mice. Cotreatment with GSH100 and tempol reversed lipid-infused insulin resistance in skeletal muscle. However, GSH alone did not prevent skeletal muscle insulin resistance (Fig. 4).

These results suggest that cotreatment with GSH100 and tempol prevents whole body and skeletal muscle insulin resistance by lipid infusion.

Cotreatment of mice with GSH and tempol significantly increased the levels of GSH or GSH/GSSG ratio compared with control mice in the lipid-infused group, although neither GSH nor GSH with tempol significantly increased both factors compared with control mice in the saline-infused group (Fig. 5). The gene expression of TNF-α in skeletal muscle was not significantly changed by either lipid infusion or antioxidants. As we have already shown that lipid infusion increased mRNA expression of TNF-α in the time course study, we speculate that unaltered mRNA levels of TNF-α in this experiment may be caused by a time dependent effect since gene expression was measured at 4 h after lipid infusion. Lipid-infusion significantly increased IL-6 mRNA expression in the skeletal muscle. Cotreatment with GSH100 and tempol reversed the lipid-infused increase in IL-6 mRNA expression, although GSH alone had no effect (Fig. 5). We also measured the activities of the MAPK family but did not find any significant changes (data not shown). Since the phosphorylation of JNK was increased at 0.5 h after lipid infusion that was returned to normal at 1 h (Fig. 1), it may be hard to detect any changes at 4 h after lipid infusion. Taken together, these results suggest that GSH with tempol prevents insulin resistance, oxidative stress, and the inflammatory response induced by lipid infusion.

Discussion

The present study showed that the lipid infusion-induced oxidative stress and insulin resistance in skeletal muscle was prevented by cotreatment with GSH and tempol. Increased lipid-induced inflammatory response was also reversed by these antioxidants.

In spite of a contradiction as to the role of ROS in glucose metabolism in skeletal muscle, antioxidants have been shown to improve whole body insulin sensitivity and beta cell function. Antioxidant *N*-acetylcysteine abolished hyperglycemia-induced insulin resistance and attenuated diabetes in Zucker fatty rats due to its effect on preservation of beta cell mass (30). Infusion of GSH partially prevented lipid-induced whole body insulin resistance (6). However, few studies have investigated the effect of antioxidants on insulin resistance in skeletal muscle. Here we showed that antioxidants also attenuated skeletal muscle insulin resistance induced by lipid infusion. Our results also support the notion that oxidative stress impairs skeletal muscle insulin resistance. The mitochondrial electron transport chain is the main source of O^{-}_{2} in skeletal muscle (31). The production of O^{-}_{2} in mitochondria is regulated by Mn-SOD that converts O^{-}_{2} into H_2O_2. The importance of Mn-SOD in mitochondria is indicated by the fact that knock-out mice without a gene for Mn-SOD show a lethal phenotype (32). In spite of the importance of SOD against ROS in mitochondria, however, treatment of mice with the SOD mimetic tempol increased oxidative stress and did not prevent lipid-induced insulin resistance. The prooxidant effect of tempol was also supported by the fact that coinfusion with tempol and lipid exaggerated cytokine expression. Previously it has also been known that SOD mimetics are known to function as either antioxidants or prooxidants depending on the experimental conditions (33). Tempol treatment induced oxidative stress and impaired mitochondrial function in vascular endothelial and smooth muscle cells (34), while treatment with tempol in drinking water reduces oxidative stress in obese Zucker rats (35). The exact mechanism of this prooxidant effect of tempol in our study is not known, but we speculate that increased accumulation of H_2O_2 may cause oxidative stress. This theory is supported by our finding that cotreatment with tempol and GSH prevented insulin resistance. A previous study also supports our speculation that treatment with tempol increased H_2O_2, leading to vasorelaxation in rat mesenteric vessels that was reversed by catalase treatment (36).

GSH is one of the major antioxidants in cells (37) and reduces free radicals not only by non-enzymatic reactions, but also in conjunction with GPx (38). A deficiency of GPx induces many detrimental effects in various tissues and animal models (39, 40). We also showed that acute lipid infusion reduced GSH concentration in skeletal muscles. Furthermore, GSH treatment increased GSH level in skeletal muscle in a dose-dependent manner, and oxidative stress by lipid fusion tended to be reversed by GSH treatment. However, GSH did not prevent whole body and skeletal muscle insulin resistance. Inconsistent with our study, GSH was previously observed to prevent whole body insulin resistance induced by 10% lipid–infusion in humans, although skeletal muscle insulin sensitivity was not measured (6). Currently, the basis of these inconsistent results is unclear, although it is conceivable that the basis may be differences in lipid dosage or experimental species.

In contrast, co-treatment with GSH and tempol effectively reversed lipid-induced oxidative stress and insulin resistance in the whole body and skeletal muscle. As mentioned above, both SOD and GPx are critical scavengers of ROS. Namely, tempol is a scavenger for O^{-}_{2} and GSH inactivates H_2O_2. Therefore, it seems that the activations of SOD and GPx rather than SOD or

GSH alone are an effective way to reverse insulin resistance in skeletal muscle. Consistent with our study, combinations of two antioxidants more effectively reduced oxidative stress than a sole antioxidant in previous studies (41 – 43).

Inflammatory cytokines are expressed not only in adipose tissue but also in skeletal muscle and exert autocrine, paracrine, and endocrine effects (44). Recent evidences suggest that inflammatory cytokines and signaling pathways are involved in skeletal muscle insulin resistance (45, 46). Acute elevation of FFAs also increases inflammatory cytokines in skeletal muscle cells and tissues (47, 48). Consistent with previous studies, the gene expressions of TNF-α and IL-6 increased in the skeletal muscle of lipid-infused mice in our time-course experiment. Furthermore, cotreatment with GSH and tempol inhibited the increase of IL-6 mRNA levels by lipid. These results suggest an inflammatory response might be modulated by oxidative stress.

Overall, lipid-infusion induced insulin resistance in skeletal muscle that was followed by oxidative stress and an increased inflammatory response. While tempol alone functioned as a prooxidant and GSH had no effect on insulin resistance, cotreatment with tempol and GSH inhibited insulin resistance and the inflammatory response by acute lipid infusion. These results suggest that oxidative stress is responsible for insulin resistance in the skeletal muscle of acute lipid-infused mice. Thus, modulation of oxidative stress may provide an effective treatment for acute lipid-induced insulin resistance in skeletal muscle.

Acknowledgments

This work was supported by the Korea Science and Engineering Foundation (KOSEF) through the Aging-Associated Vascular Disease Research Center at Yeungnam University (R13-2005-005-01003-0) and also supported by a Korea Research Foundation Grant funded by the Korean Government (MOEHRD) (KRF-2006-531-E00004).

References

1 Baron AD, Brechtel G, Wallace P, Edelman SV. Rates and tissue sites of non-insulin- and insulin-mediated glucose uptake in humans. Am J Physiol. 1988;255:E769–E774.

2 DeFronzo RA, Jacot E, Jequier E, Maeder E, Wahren J, Felber JP. The effect of insulin on the disposal of intravenous glucose. Results from indirect calorimetry and hepatic and femoral venous catheterization. Diabetes. 1981;30:1000–1007.

3 Park SY, Cho YR, Kim HJ, Higashimori T, Danton C, Lee MK, et al. Unraveling the temporal pattern of diet-induced insulin resistance in individual organs and cardiac dysfunction in C57BL/6 mice. Diabetes. 2005;54:3530–3540.

4 Kahn SE, Hull RL, Utzschneider KM. Mechanisms linking obesity to insulin resistance and type 2 diabetes. Nature. 2006; 444:840–846.

5 Kim JK, Kim YJ, Fillmore JJ, Chen Y, Moore I, Lee J, et al. Prevention of fat-induced insulin resistance by salicylate. J Clin Invest. 2001;108:437–446.

6 Paolisso G, Gambardella A, Tagliamonte MR, Saccomanno F, Salvatore T, Gualdiero P, et al. Does free fatty acid infusion impair insulin action also through an increase in oxidative stress? J Clin Endocrinol Metab. 1996;81:4244–4248.

7 Oakes ND, Cooney GJ, Camilleri S, Chisholm DJ, Kraegen EW. Mechanisms of liver and muscle insulin resistance induced by chronic high-fat feeding. Diabetes. 1997;46:1768–1774.

8 Thamer C, Haap M, Bachmann O, Zur Nieden T, Tschritter O, Stefan N, et al. Serum adiponectin levels predict the effect of short-term dietary interventions on insulin sensitivity in humans. Diabetologia. 2004;47:1303–1305.

9 Watt MJ, Hevener A, Lancaster GI, Febbraio MA. Ciliary neurotrophic factor prevents acute lipid-induced insulin resistance by attenuating ceramide accumulation and phosphorylation of c-Jun N-terminal kinase in peripheral tissues. Endocrinology. 2006;147:2077–2085.

10 Randle PJ, Garland PB, Hales CN, Newsholme EA. The glucose fatty-acid cycle. Its role in insulin sensitivity and the metabolic disturbances of diabetes mellitus. Lancet. 1963;1:785–789.

11 Krebs M, Roden M. Molecular mechanisms of lipid-induced insulin resistance in muscle, liver and vasculature. Diabetes Obes Metab. 2005;7:621–632.

12 Evans JL, Maddux BA, Goldfine ID. The molecular basis for oxidative stress-induced insulin resistance. Antioxid Redox Signal. 2005;7:1040–1052.

13 Kim JE, Kim YW, Lee IK, Kim JY, Kang YJ, Park SY. AMP-activated protein kinase activation by 5-aminoimidazole-4-carboxamide-1-beta-D-ribofuranoside (AICAR) inhibits palmitate-induced endothelial cell apoptosis through reactive oxygen species suppression. J Pharmacol Sci. 2008;106:394–403.

14 Xiao C, Giacca A, Lewis GF. Oral taurine but not N-acetylcysteine ameliorates NEFA-induced impairment in insulin sensitivity and beta cell function in obese and overweight, non-diabetic men. Diabetologia. 2008;51:139–146.

15 Evans JL, Goldfine ID, Maddux BA, Grodsky GM. Oxidative stress and stress-activated signaling pathways: a unifying hypothesis of type 2 diabetes. Endocr Rev. 2002;23:599–622.

16 Sandstrom ME, Zhang SJ, Bruton J, Silva JP, Reid MB, Westerblad H, et al. Role of reactive oxygen species in contraction-mediated glucose transport in mouse skeletal muscle. J Physiol. 2006;575:251–262.

17 Higaki Y, Mikami T, Fujii N, Hirshman MF, Koyama K, Seino T, et al. Oxidative stress stimulates skeletal muscle glucose uptake through a phosphatidylinositol 3-kinase-dependent pathway. Am J Physiol Endocrinol Metab. 2008;294:E889–E897.

18 Aydin A, Orhan H, Sayal A, Ozata M, Sahin G, Isimer A. Oxidative stress and nitric oxide related parameters in type II diabetes mellitus: effects of glycemic control. Clin Biochem. 2001;34: 65–70.

19 Matsushima S, Kinugawa S, Ide T, Matsusaka H, Inoue N, Ohta Y, et al. Overexpression of glutathione peroxidase attenuates myocardial remodeling and preserves diastolic function in diabetic heart. Am J Physiol Heart Circ Physiol. 2006;291: H2237–H2245.

20 Kim JA, Wei Y, Sowers JR. Role of mitochondrial dysfunction

in insulin resistance. Circ Res. 2008;102:401–414.
21 Cheung PY, Wang W, Schulz R. Glutathione protects against myocardial ischemia-reperfusion injury by detoxifying peroxynitrite. J Mol Cell Cardiol. 2000;32:1669–1678.
22 Meister A, Anderson ME. Glutathione. Annu Rev Biochem. 1983;52:711–760.
23 Hussein KS, Jones BE. Effects of selenium administration on erythrocyte and blood plasma glutathione peroxidase activity in goats. Acta Vet Scand. 1982;23:559–564.
24 Chess DJ, Xu W, Khairallah R, O'Shea KM, Kop WJ, Azimzadeh AM, et al. The antioxidant tempol attenuates pressure overload-induced cardiac hypertrophy and contractile dysfunction in mice fed a high-fructose diet. Am J Physiol Heart Circ Physiol. 2008;295:H2223–H2230.
25 Kugiyama K, Miyao Y, Sakamoto T, Kawano H, Soejima H, Miyamoto S, et al. Glutathione attenuates coronary constriction to acetylcholine in patients with coronary spastic angina. Am J Physiol Heart Circ Physiol. 2001;280:H264–H271.
26 Zhang QS, Eaton L, Snyder ER, Houghtaling S, Mitchell JB, Finegold M, et al. Tempol protects against oxidative damage and delays epithelial tumor onset in Fanconi anemia mice. Cancer Res. 2008;68:1601–1608.
27 Park SY, Kim HJ, Wang S, Higashimori T, Dong J, Kim YJ, et al. Hormone-sensitive lipase knockout mice have increased hepatic insulin sensitivity and are protected from short-term diet-induced insulin resistance in skeletal muscle and heart. Am J Physiol Endocrinol Metab. 2005;289:E30–E39.
28 Weintraub M, Rassin T, Eisenberg S, Ringel Y, Grosskopf I, Iaina A, et al. Continuous intravenous heparin administration in humans causes a decrease in serum lipolytic activity and accumulation of chylomicrons in circulation. J Lipid Res. 1994;35:229–238.
29 Hennes MM, Dua A, Kissebah AH. Effects of free fatty acids and glucose on splanchnic insulin dynamics. Diabetes. 1997;46:57–62.
30 Kaneto H, Kajimoto Y, Miyagawa J, Matsuoka T, Fujitani Y, Umayahara Y, et al. Beneficial effects of antioxidants in diabetes: possible protection of pancreatic beta-cells against glucose toxicity. Diabetes. 1999;48:2398–2406.
31 Muller FL, Liu Y, Van Remmen H. Complex III releases superoxide to both sides of the inner mitochondrial membrane. J Biol Chem. 2004;279:49064–49073.
32 Li Y, Huang TT, Carlson EJ, Melov S, Ursell PC, Olson JL, et al. Dilated cardiomyopathy and neonatal lethality in mutant mice lacking manganese superoxide dismutase. Nat Genet. 1995;11:376–381.
33 Aronovitch Y, Godinger D, Israeli A, Krishna MC, Samuni A, Goldstein S. Dual activity of nitroxides as pro- and antioxidants: catalysis of copper-mediated DNA breakage and H2O2 dismutation. Free Radic Biol Med. 2007;42:1317–1325.
34 Alpert E, Altman H, Totary H, Gruzman A, Barnea D, Barash V, et al. 4-Hydroxy tempol-induced impairment of mitochondrial function and augmentation of glucose transport in vascular endothelial and smooth muscle cells. Biochem Pharmacol. 2004;67:1985–1995.
35 Banday AA, Marwaha A, Tallam LS, Lokhandwala MF. Tempol reduces oxidative stress, improves insulin sensitivity, decreases renal dopamine D1 receptor hyperphosphorylation, and restores D1 receptor-G-protein coupling and function in obese Zucker rats. Diabetes. 2005;54:2219–2226.
36 Chen Y, Pearlman A, Luo Z, Wilcox CS. Hydrogen peroxide mediates a transient vasorelaxation with tempol during oxidative stress. Am J Heart Circ Physiol. 2007;293:H2085–H2092.
37 Santangelo F, Witko-Sarsat V, Drueke T, Descamps-Latscha B. Restoring glutathione as a therapeutic strategy in chronic kidney disease. Nephrol Dial Transplant. 2004;19:1951–1955.
38 Zeevalk GD, Razmpour R, Bernard LP. Glutathione and Parkinson's disease: is this the elephant in the room? Biomed Pharmacother. 2008;62:236–249.
39 Torzewski M, Ochsenhirt V, Kleschyov AL, Oelze M, Daiber A, Li H, et al. Deficiency of glutathione peroxidase-1 accelerates the progression of atherosclerosis in apolipoprotein E-deficient mice. Arterioscler Thromb Vasc Biol. 2007;27:850–857.
40 Klivenyi P, Andreassen OA, Ferrante RJ, Dedeoglu A, Mueller G, Lancelot E, et al. Mice deficient in cellular glutathione peroxidase show increased vulnerability to malonate, 3-nitropropionic acid, and 1-methyl-4-phenyl-1,2,5,6-tetrahydropyridine. J Neurosci. 2000;20:1–7.
41 Zal F, Mostafavi-Pour Z, Vessal M. Comparison of the effects of vitamin E and/or quercetin in attenuating chronic cyclosporine A-induced nephrotoxicity in male rats. Clin Exp Pharmacol Physiol. 2007;34:720–724.
42 Bowry VW, Mohr D, Cleary J, Stocker R. Prevention of tocopherol-mediated peroxidation in ubiquinol-10-free human low density lipoprotein. J Biol Chem. 1995;270:5756–5763.
43 Atasayar S, Gurer-Orhan H, Orhan H, Gurel B, Girgin G, Ozgunes H. Preventive effect of aminoguanidine compared to vitamin E and C on cisplatin-induced nephrotoxicity in rats. Exp Toxicol Pathol. 2009;61:23–32.
44 Pedersen BK, Akerstrom TC, Nielsen AR, Fischer CP. Role of myokines in exercise and metabolism. J Appl Physiol. 2007;103:1093–1098.
45 Kraegen EW, Cooney GJ. Free fatty acids and skeletal muscle insulin resistance. Curr Opin Lipidol. 2008;19:235–241.
46 Wei Y, Chen K, Whaley-Connell AT, Stump CS, Ibdah JA, Sowers JR. Skeletal muscle insulin resistance: role of inflammatory cytokines and reactive oxygen species. Am J Physiol Regul Integr Comp Physiol. 2008;294:R673–R680.
47 Fabris R, Nisoli E, Lombardi AM, Tonello C, Serra R, Granzotto M, et al. Preferential channeling of energy fuels toward fat rather than muscle during high free fatty acid availability in rats. Diabetes. 2001;50:601–608.
48 Weigert C, Brodbeck K, Staiger H, Kausch C, Machicao F, Haring HU, et al. Palmitate, but not unsaturated fatty acids, induces the expression of interleukin-6 in human myotubes through proteasome-dependent activation of nuclear factor-kappaB. J Biol Chem. 2004;279:23942–23952.